ELSEVIER

International Journal of Mass Spectrometry 190/191 (1999) 59–68

International Journal of Mass Spectrometry

A dual quadrupole ion trap mass spectrometer

Y. Zerega*, P. Perrier, M. Carette, G. Brincourt, T. Nguema, J. Andre

Université de Provence, IUSTI-GIPSE (U.M.R. n° 6595), Technopôle de Chateau Gombert, F 13453 Marseille Cedex 13, France

Received 28 September 1998; accepted 31 December 1998

Abstract

Two quadrupole ion traps are used to carry out a mass spectrometer. The first concerns ion preparation with possible mass selection functions. The second is used as a mass analysis cell to obtain the secular frequency of simultaneously confined ions. After ion ejection, the secular frequencies are computed from the evolution of time-of-flight (TOF) histograms. Comments and results concerning the ion preparation are given. Then, the metrological parameters of the mass spectrometer prototype are examined: amplitude calibration, visibility, resolution, and mass range. (Int J Mass Spectrom 190/191 (1999) 59–68) © 1999 Elsevier Science B.V.

Keywords: Quadrupole ion trap; Secular frequency; Fourier analysis; Mass spectrometry

1. Introduction

The Paul trap is the major research theme of our team. Since 1971 the team has researched confined ions statistics and later experimentally studied the relaxation of negative molecular ions created by charge exchange with excited Rydberg atoms: X**. In this manner, we can obtain electrons with precisely defined energy during charge exchange and that are less perturbed by electric fields than free electrons.

The lifetime of SF_6^- molecular ions was studied versus the X** atom quantum level selected by electronic excitation followed by laser excitation [1].

For these lifetime measures, the trap was used as a confinement cell. Externally created SF_6^- ions were introduced in the cell and then confined for a given time. The number of confined ions at the end of this time was measured by ejection of all the particles. A dc dipolar electric field led the ions toward an electron multiplier where they were counted. This measure was destructive, so the experiment was repeated for different confinement time intervals to build a temporal ion signal. Because of the trap apparatus function (ion trap loss processes) and intrinsic ion lifetime, a decrease in the temporal curves was observed.

On these curves, periodic low amplitude oscillation was noted. After a critical analysis of the operating mode, the Fourier transform of this ion signal revealed that the frequency of these oscillations corresponded to the axial secular frequency of the SF_6^- ions in the experimental conditions. The discrimination of the ejected ions versus their position and velocity at the end of the confinement was an unexpected phenomenon, and gave rise to a new operating mode of a quadrupole ion trap for mass analysis [2,3]. And so, encouraged by March [4,5], a new line of research was developed in the laboratory.

* Corresponding author. E-mail: yzerega@iusti.univ-mrs.fr

Dedicated to J.F.J. Todd and R.E. March in recognition of their original contributions to quadrupole ion trap mass spectrometry.

PII S1387-3806(99)00005-6

2. Experimental apparatus

The mass spectrometer consists of an ion preparation cell and a mass analysis cell.

The mass analysis cell is a pure quadrupole ion trap (noted T2) using our nonconventional operating mode. This operating mode allows the secular frequencies of simultaneously confined ions to be measured by trajectory analysis. So, the pressure must be very low ($\sim 10^{-7}$ Torr) in the mass analysis cell to have the smallest possible number of collisions between the ions and the residual vacuum gas in order to prevent ionic trajectory perturbations.

The ion preparation cell requires gas inlets and so the pressure must be higher ($\sim 10^{-4}$ Torr) in this cell than in that of the mass analysis. Consequently, the two cells are located in different vacuum chambers separated by a small hole for ion transfer. The separation of these two functions (preparation and mass analysis) was first proposed by Lawson et al. by coupling a QUISTOR with a quadrupole mass filter for the study of ion reactions [6–8]. The ion preparation cell consists of a second pure quadrupole ion trap (noted T1) for mass selection and enrichment of selected ionic species. This is necessary for (1) a small chemical quantity to be analyzed, and (2) reactions with low creation rates. Moreover, in T1 the ions are cooled in the center in order to optimize (1) the quantity of the ions transferred from T1 to T2 (reduction of the radial spread of the ion cloud), and (2) the acceptance of the ions by the confinement field in T2 (reduction of the axial spread of the ion cloud).

The general device and the temporal variation in the potentials applied to the electrodes (or scan function) are shown in Figs. 1 and 2, respectively. The different operating steps of the device are described chronologically.

The preparation step is carried out in trap T1 where the ions are created. Here (Fig. 1) a device concerning the creation of positive ions by electron impact (EI) is represented. To test the metrological properties of the apparatus we use Xenon gas, which has an interesting natural isotopic composition. During the creation (step A), the electron gun (EG) is turned on and the ions are submitted to the electric confinement field generated by a constant maximal amplitude confinement voltage $U_{01} + V_{01} \cos \Omega t$ applied to the ring electrode R1, the upper endcap UEC1, and the lower endcap LEC1 being grounded. During creation ion confinement allows the total number of ions to be increased at the end of the creation step (enrichment). During the preparation (step B) the ions are submitted to the confinement field and to collisions with buffer Helium gas to cool them toward the center of the trap, by losing kinetic energy [9]. The size of the ion cloud is then reduced to maximize the number of ions transferred from T1 to T2 for mass analysis. Moreover, to eliminate undesirable ionic species, we could make a *m/z* selection by tuning the amplitude of the confinement voltages (by moving the trap working point) as illustrated in Sec. 3.1. We could also incorporate other mass selection methods that are used in commercial instruments, for instance, by mono- or multifrequency resonant ejections [10–12].

The transfer step (step C) starts with the ejection of the positive ions out of T1 through a small hole. The confinement voltage applied to R1 is turned off. A positive and a negative dc voltage are applied to LEC1 and to UEC1, respectively, to generate a dipolar electric field. The transfer cell is a simple flight tube on which a dc voltage of -250 V is continuously applied. The ions are accelerated at the exit of T1, then slowed down between the flight tube and the trap T2. A negative and a positive dc voltage is applied to LEC2 and to UEC2, respectively, to generate a dipolar electric field in T2 in order to stop the positive ions in a decentered axial position $z(t_0)$. The transfer time must be as short as possible to minimize the radial position scattering of the ionic cloud with the intention of transferring the maximum number of ions into T2. For negative ion transfer the polarity of the dc voltages applied to the endcaps and to the flight tube is reversed.

The mass analysis step is performed in trap T2. The slowing down of the ions in trap T2 is adjusted so that the ions have a sufficiently low velocity and a decentered initial position to be confined with a significant axial motion amplitude. The ions are confined by applying an alternative voltage $U_{02} + V_{02} \cos \Omega t$ between the ring R2 and the two endcaps of

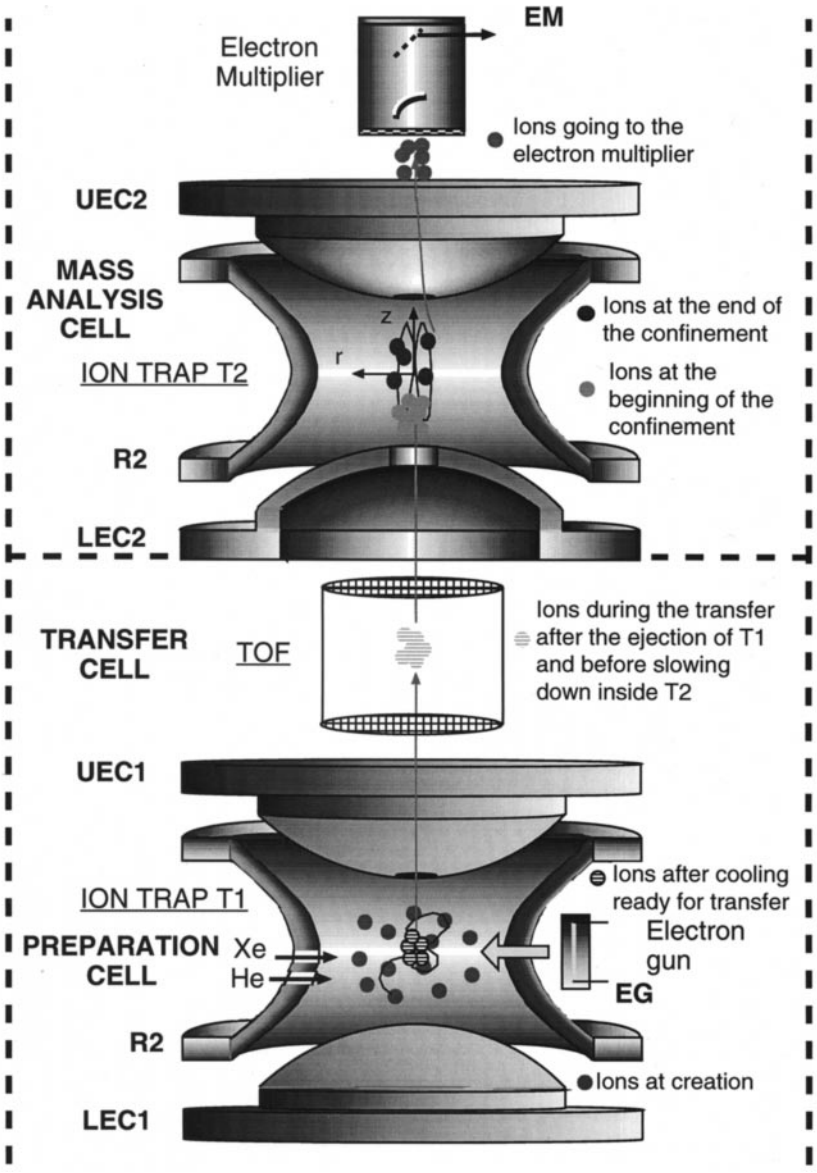

Fig. 1. General structure of the mass spectrometer. The electrodes of the device are: LEC1 for lower endcap of T1, R1 for ring of T1, UEC1 for upper endcap of T1, LEC2 for lower endcap of T2, R2 for ring of T2, and UEC2 for upper endcap of T2. The amplified analog signal coming from the electron multiplier is noted EM, and the polarization of the electron gun is noted EG.

T2. The amplitudes U_{02} and V_{02} are constant during the entire experiment. At the end of the confinement, a dipolar field ejects the ions from the trap T2 toward the electron multiplier by applying a positive dc voltage to LEC2, the lower endcap of T2, and a negative dc voltage to UEC2, the upper endcap of T2. Information concerning ion time-of-flight (TOF) signals is recorded from the amplified analog signal coming from the electron multiplier (EM). Either the TOF signal is digitized and recorded, or the number of ions in a counting gate (time interval F) is summed and recorded.

The mass analysis principle and signal data process relating to the operating mode will be discussed in Sec. 3.2.

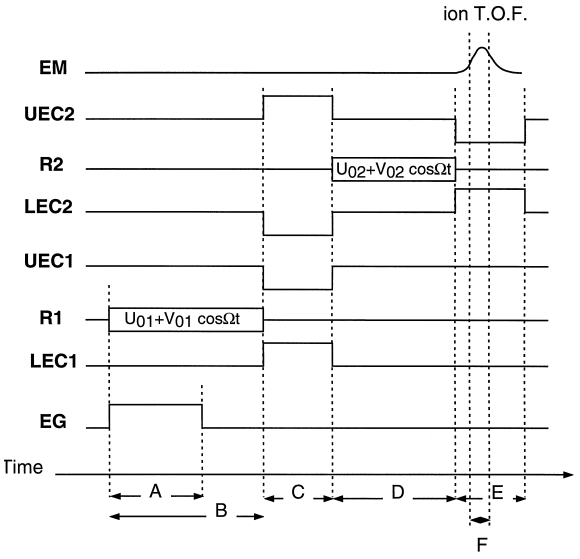

Fig. 2. Scan function of the operating mode of the mass spectrometer for one elementary experiment. The steps are referenced A for the ion creation, B for the ion preparation confinement time in T1 (cooling and enrichment), C for the transfer from T1 to T2, D for the confinement time for mass analysis, E for the ejection out of T2, and F for the counting gate.

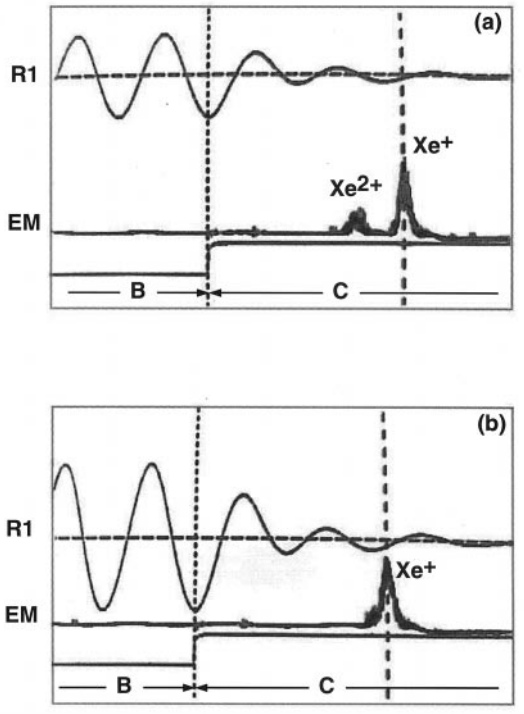

Fig. 3. Xe^+ and Xe^{2+} ions TOF detection for a direct transfer from T1 to the detector and for an electron impact of 100 eV. The maximum amplitude of the alternative confinement voltage is equal to (a) 57 V, and (b) 100 V. The voltage applied to the ring electrode of T1 is noted R1 and the amplified analog signal coming from the electron multiplier is noted EM. The signals are represented at the end of the preparation step (B) and at the beginning of the transfer step (C).

3. Results and discussion

3.1. Ion preparation and transfer

In order to study the parameters affecting the ion preparation and the transfer process, dc potentials are applied to the electrodes of the ion trap T2 and are set to −150 V. Under these conditions, the analysis cell behaves as a flight tube. Ions are transferred from T1 to T2 without any significant perturbations of their trajectories and they are detected by the electron multiplier.

The ionization of Xenon is achieved in T1 by an electron impact of about 100 eV. At this energy level it is possible to create Xe^+ and Xe^{2+} ions [13] as shown in Fig. 3(a). We can observe the two TOF distributions after ejection from T1; the first one corresponds to Xe^{2+} ions and the second one to Xe^+ ions. The value of the maximum amplitude of the alternative confinement voltage can be increased such that Xe^{2+} ions are not confined [Fig. 3(b)].

The speed of ion cooling in T1 depends on the mass, the temperature, and the partial pressure of the He neutral gas (“thermal bath”); it also depends on the mass, the initial translation energy, and the secular frequency of the ions. It is important to note that the equilibrium temperature reached is always higher than the neutral gas temperature in a ratio between 1:1 and 3:1 [14].

Experimental results concerning Xe^+ ion cooling are given in Fig. 4. The curve expresses the number of detected ions versus confinement time in T1 after a creation time of 1 ms. The increasing number of detected ions at the beginning shows the efficiency of the cooling. The standard deviations of the velocity and spatial distributions of the ion cloud decrease with time, so the number of transmitted (and thus detected) ions passing through the hole of the upper endcap of

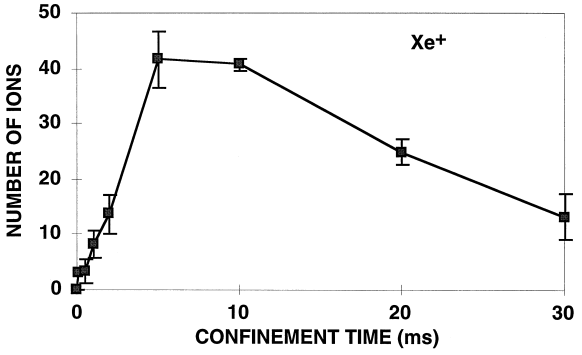

Fig. 4. Number of Xe^+ ions detected for a direct transfer from T1 to the detector vs. the confinement time after a creation time of 1 ms.

T1 increases even after the end of the ion creation. The maximum of the curve gives a cooling time of about 5 ms. This value is in agreement with the one deduced from simulation studies [15] within the context of our experimental conditions. The decreasing of the curve (Fig. 4) shows the cooling process reaches the saturation point (in the experimental conditions) and the losing processes (because, for example, of the atomic beams) prevail and the detected number of ions decreases.

3.2. Mass analysis

For a better comprehension of this nonconventional operating mode, this paragraph summarizes previously published works concerning the mass analysis operating mode of a quadrupole ion trap.

3.2.1. Probing axial secular frequency

Let us consider $(x(t_i), y(t_i), z(t_i))$ and $(x'(t_i), y'(t_i), z'(t_i))$, respectively the position and the velocity components of an ion at the confinement time t_i. The latter is defined as

$$t_i = iT_e \text{ (with } i = 1 \text{ to } N_c) \tag{1}$$

where T_e is the sample period of the signal and N_c is the total number of confinement times or confinement time channels.

At this time t_i, if the confinement field is replaced by a dc dipolar field that ejects the ion toward the upper endcap of the trap, the TOF $t_f(t_i)$ to reach the upper endcap is given by the relation

$$t_f(t_i) = \frac{1}{A}\left[-z'(t_i) + \sqrt{z'^2(t_i) - 2A(z(t_i) - z_0)}\right] \tag{2}$$

with

$$A = \frac{Z \cdot e \cdot U_e}{m \cdot m_u \cdot z_0}$$

and where m is the ion mass in u; m_u is the unified atomic mass in kg; Z is the charge number (negative or positive according to the ion charge); e is the elementary charge in C; z_0 is the shortest distance in m between the center of the trap and the endcaps; and U_e is the amplitude of the ejection dc dipolar potential in V.

The TOF depends on the ion axial position $z(t_i)$ and the ion axial velocity $z'(t_i)$. So, the Fourier transform (spectrum) of the function "time of flight" $t_f(t_i)$ gives the frequencies of ion motion for the ion ejected. We sample this signal at the period T_e a whole multiple of the micrometric motion $T_\Omega = 2\pi/\Omega$:

$$T_e = jT_\Omega, \ (j \text{ belongs to } \mathbb{N}^*) \tag{3}$$

In this case, the spectrum contains only the information on axial secular frequency of the confined ion.

3.2.2. The complete experiment

The elementary experiment previously described in Sec. 2 is destructive for the ion cloud unlike other Fourier transform quadrupole ion trap operating modes [16–18]. In order to obtain a signal versus confinement time, the steps of this elementary experiment must be repeated for different increasing confinement times from T_e to T_m, the maximum confinement time defined by

$$T_m = N_c T_e = N_c j T_\Omega \tag{4}$$

Although the ion signal is obtained from N_c separate elementary experiments, this signal is consistent because all the elementary experiments are perfectly

reproducible when all the driving pulsed electronic signals are phase locked.

If the number of created ions is statistically very low (less than one ion), it is possible to repeat each elementary experiment having the same confinement time and superimpose the results of each confinement time.

Currently, the total experimental time can be expressed by the relation

$$T_{\text{exp}} = (T_p + T_m/2)\, N_c M \quad (5)$$

where T_p is the duration of the preparation step (step B) and M is the number of repetitions of each elementary experiment related to the same confinement time. For example, to obtain a mass resolution of about 1000 with the experimental conditions given in Table 2, $T_{\text{exp}} \approx (5 + 16/2)*256*20 \approx 66$ s.

3.2.3. How to obtain the TOF information

In the case of only one confined species, for each confinement time we collect an ion TOF distribution induced by the velocity and position distributions of the ion cloud at the beginning of the confinement. When the elementary experiment is repeated M times, the superimposition of each elementary TOF distribution, at each confinement time, gives the same distribution as that obtained by conducting only one elementary experiment with the superimposition of the ions clouds at the beginning of the confinement. Depending on the confinement time, the TOF distributions evolve at the secular period of the confined species. From these TOF distributions, we deduce the number of ions and the secular frequency leading to *m/z*.

For different confined species depending on *m/z*, the shape of the TOF distributions becomes more complex. Indeed, each species evolves with its own value of secular frequency and number of ions. Fig. 5 gives a set of experimental TOF distributions concerning Xe^+ isotopic ions.

We do not have a simple function of the TOF information, on the one hand because of position and velocity distributions of the ionic cloud at the beginning of the confinement and, on the other hand, because of a superimposition of the TOF information that evolves at different frequencies depending on the species. Moreover, the TOF information does not allow the ion quantity to be measured according to each species.

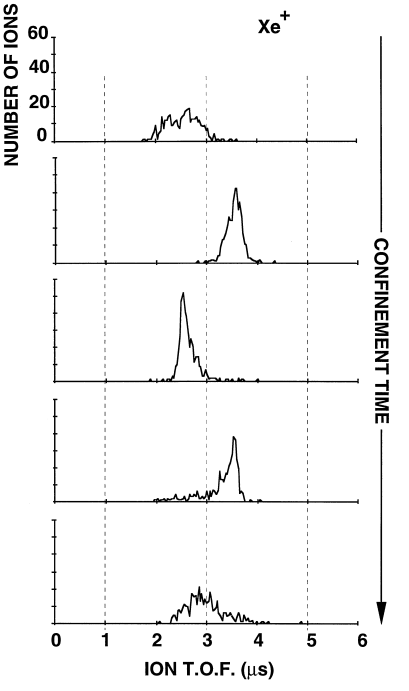

Fig. 5. Experimental TOF distributions for five consecutive confinement times concerning Xe^+ isotopic ions [19].

In order to attain a spectrum image of the secular frequency and the number of ions for each species, we discriminate the TOF. A temporal ion signal versus confinement time is established within each confinement time; the number of ions arriving in the same given TOF range is summed.

In Fig. 6 the ion signal for SF_6^- obtained by integrating the number of ions measured by a counting gate in a TOF range is shown versus the confinement time. The signal reveals (1) an oscillation of the number of detected ions, which is characteristic of the axial secular frequency of the SF_6^- ions, and (2) an overall decrease in the number of ions attributed to the intrinsic lifetime of the SF_6^- ions and to a relaxation of the ionic motion by collision with the residual gas.

3.2.4. Signal data processing

The best position and width of the TOF range of discrimination must be determined. Indeed, depending

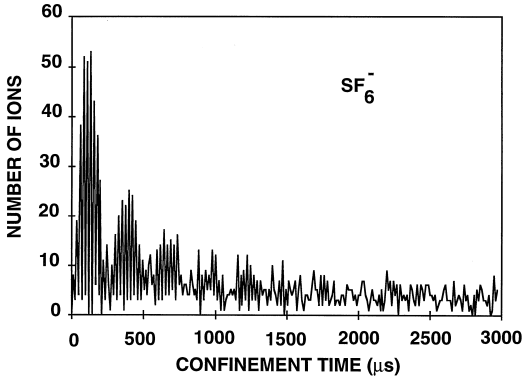

Fig. 6. Number of SF_6^- ions vs. confinement time detected inside a selected TOF range [19].

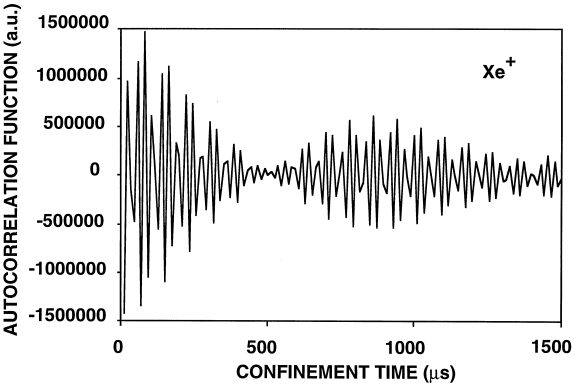

Fig. 7. Autocorrelation function vs. confinement time for Xe^+ isotopic ions [19].

on a given position and width of this TOF range, different results are obtained with respect to the spectrum amplitude and the shape of the detected temporal signal [19]. This method of TOF selective detection gives satisfactory results but it is difficult to have a dynamic optimum and the most sinusoidal signal possible.

So, we propose another detection method in which we record the whole of the TOF information and we obtain a TOF histogram for each confinement time by data processing. The total TOF range can be divided into smaller TOF ranges. The dynamic optimum with the most sinusoidal signal possible is obtained for two TOF ranges, as shown in Fig. 5 by the broken lines. Then we build two ion signals versus the confinement time by totaling the number of ions in each band. To obtain an overall temporal signal, we use the autocorrelation function of each signal to avoid phase problems and we sum these two functions (see Fig. 7). Then, we take the real Fourier transform to obtain the power spectrum (see Fig. 8) containing the axial secular frequencies of the simultaneously confined species. We can also take the power spectrum of each temporal signal and sum them—that gives the same result.

3.3. Metrology of the parameters

We examine the principal metrological parameters of the device and we compare the experimental results with the simulated and the analytical ones.

3.3.1. Amplitude calibration

The amplitude calibration is deduced from statistical behaviour of the device for some experiments. From five frequency spectra and for the three main isotopes of the Xenon, the mean value of the amplitude for each peak $E[A_p]$ was calculated. Knowing $E[A_p]$, the mean number of detected ions $\bar{N}$ for each isotope is expressed by the expression (see the analytical calculations leading to the expression in [20,21])

$$\bar{N} = \frac{4}{T_m}\sqrt{E[A_p]} \tag{6}$$

The amplitude calibration was made by comparing the relative experimental percentage of the three main

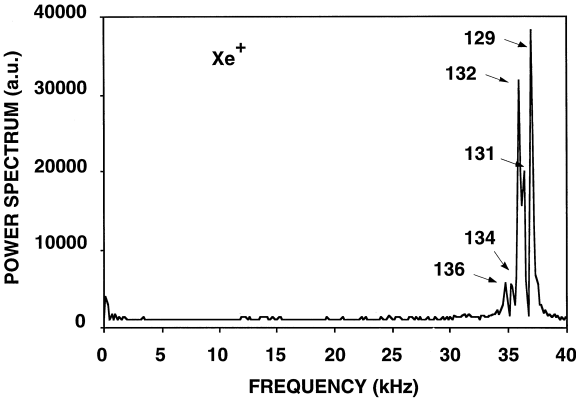

Fig. 8. Power spectrum of the signal of Fig. 4 for Xe^+ isotopic ions [19].

Table 1
Mean value of the peak amplitude $E[A_p]$, mean number of ions $\bar{N}$, experimental proportions and natural abundance, and visibility of the peak $R'_{s/n}$ for the three main isotopes of the Xenon

m/z	$E[A_p]$	$\bar{N}$	Experimental proportions (%)	Natural abundance (%)	$R'_{s/n}$
129	$6.552\ 10^{-5}$	7.9	28.34	26.24	290
131	$3.737\ 10^{-5}$	5.97	21.40	21.24	200
132	$4.961\ 10^{-5}$	6.88	24.66	26.93	275

isotopes (evaluated from the mean number of ions) with respect to the isotopic abundance. The set of the numerical values for each isotope is given in Table 1. Each experimental ionic abundance is in agreement with the theoretical one; however, a slightly greater value is observed for the lower mass.

3.3.2. Visibility

For one spectrum, we can define a visibility criterion from the ratio

$$R'_{s/n} = \frac{A_p}{\sigma[A_n]} \tag{7}$$

where A_p is the peak amplitude and $\sigma[A_n]$ is the standard deviation of background noise calculated far enough from the peaks. Generally, the value 4 is chosen for the minimum visibility threshold. The experimental results (see Table 1) give very good visibility since $R'_{s/n}$ is greater than 200.

It can be seen that these experimental results concerning amplitude calibration and visibility were obtained with a small number of ions, fewer than 10 by isotope.

3.3.3. Resolution

In Fourier transform methods, the resolution depends on the full width at half maximum of the peak. It is directly linked to the maximum observation time T_m of the temporal signal. An expression of the mass resolution is given in [22]:

$$R_m \approx 0.564\ \lambda(\beta_z)\ N_c\ j$$

with

$$\Delta\beta_z\ j \leq 1 \tag{8}$$

The mass resolution depends on the operating point through the parameter $\lambda(\beta_z)$ that was generally close to 0.6 in the experiments employed, and on the observation time through the parameters N_c and j.

So that the spectra of the different sampling orders do not overlap, we have to consider the Nyquist criterion. Generally, this criterion is applied to a frequency range from 0 to $\beta_{z\max}$ and in our case leads to the inequality $\beta_{z\max}\ j \leq 1$. If the minimum of the frequency is not zero, i.e. in the case of a mass range analysis defined by $\Delta\beta_z$, the inequality becomes $\Delta\beta_z\ j \leq 1$ as expressed in Eq. (8).

Experimental and theoretical mass resolutions are reported as a function of the parameters N_c and j in Table 2, Fig. 9 and Table 3, Fig. 10, respectively. The R_m values are in agreement. The experimental mass resolution is presently limited to 1000.

3.3.4. Mass range

Now, the device can achieve a mass analysis between 20 u and 400 u by mass ranges of about 40 u.

The operating mode induces a mass range for the three main points: (1) the mass analysis is performed for simultaneously confined ions since the maximum

Table 2
Experimental and theoretical mass resolutions for the isotope 131 vs. the maximum number of confinement time channels N_c and $j = 1$

N_c	R_m (experimental)	R_m (theoretical)
256	80	72
512	197	144
1024	303	288
2048	436	576
4096	720	1152

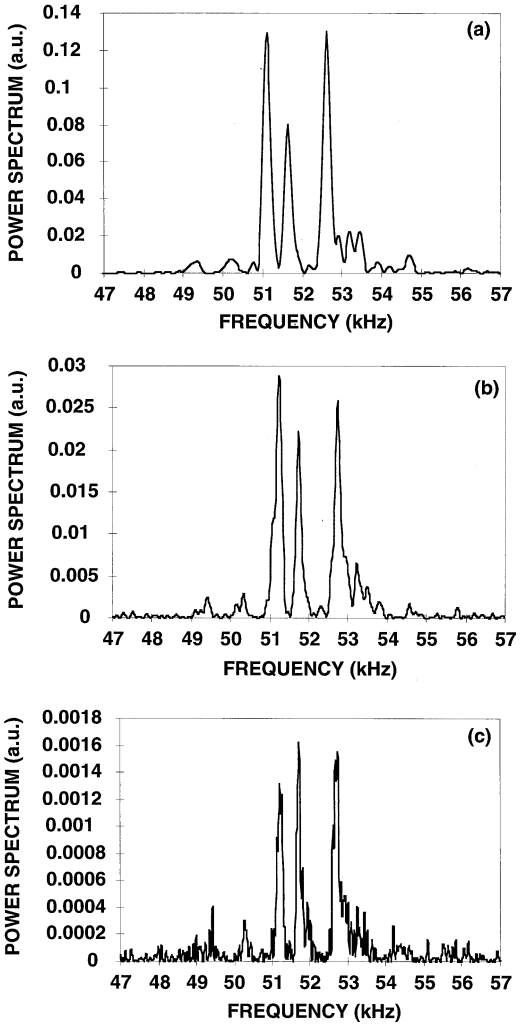

Fig. 9. Experimental power spectrum for Xe^+ isotopic ions for $j = 1$ and for (a) $N_c = 1024$, (b) $N_c = 2048$, and (c) $N_c = 4096$.

value of the amplitude of the confinement voltage is constant during mass analysis, (2) no overlapping of the sampling order frequency spectra must appear

Table 3
Experimental and theoretical mass resolutions for the isotope 132 vs. j and with the maximum number of confinement time channels $N_c = 256$

j	R_m (experimental)	R_m (theoretical)
8	528	530
16	916	1060

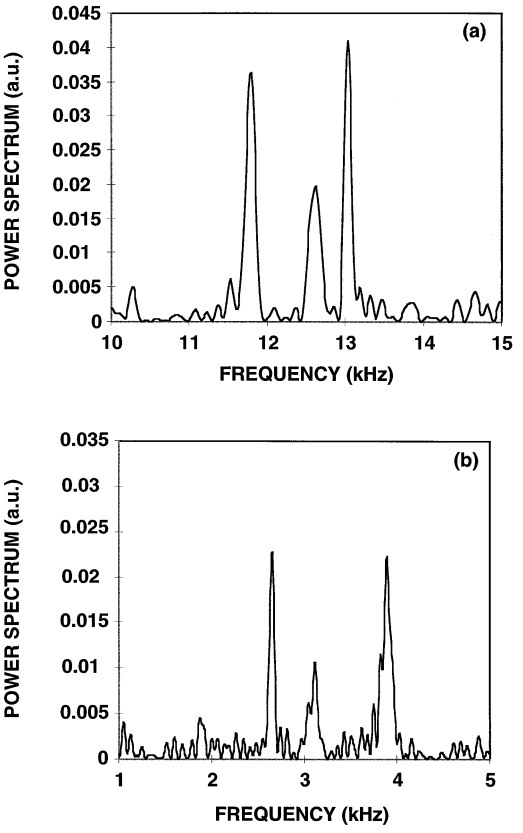

Fig. 10. Experimental power spectrum for Xe^+ isotopic ions for $N_c = 256$ and for (a) $j = 8$ and (b) $j = 16$. Power spectra are computed from zero to the Nyquist frequency. When j increases the Nyquist frequency decreases and in this frequency domain we observe peaks at apparent frequencies corresponding to the negative frequencies of sampling order greater than 0.

since the temporal signal is digitized, and (3) the current transfer cell leads to a temporal *m/z* species separation reducing the *m/z* range of the ion acceptance for mass analysis by T2.

4. Conclusion

The prototype of this mass spectrometer leads to promising results with only a few detected ions (less than 10). It gives spectra having an excellent visibility with a possible amplitude calibration and a resolution of about 1000.

We must add other ion creation devices to the

preparation cell, for example, to create negative ions by charge exchange with Rydberg atoms. The mass isolation scan functions must also be integrated. The transfer stage between the two quadrupole ion traps must be improved to increase the number of transmitted ions and the mass range. For the mass analysis stage, it is necessary to reduce the instabilities (voltages and times) of the electric generators to increase mass resolution.

Acknowledgement

The authors acknowledge the financial support of SERES.

References

[1] G. Brincourt, S. Rajab-Pacha, R. Catella, Y. Zerega, J. Andre, Chem. Phys. Lett. 156 (1989) 573.
[2] G. Brincourt, R. Catella, Y. Zerega, J. Andre, Chem. Phys. Lett. 174 (1990) 626.
[3] Y. Zerega, G. Brincourt, J. Andre, R. Catella, Int. J. Mass Spectrom. Ion Processes 121 (1992) 77.
[4] R.E. March, J.F.J. Todd, Practical Aspects of Ion Trap Mass Spectrometry, CRC Press, Boca Raton, FL, 1995, Vol. I. R.E. March, J.F.J. Todd, Practical Aspects of Ion Trap Mass Spectrometry, CRC Press, Boca Raton, FL, 1995, Vol. II. R.E. March, J.F.J. Todd, Practical Aspects of Ion Trap Mass Spectrometry, CRC, Boca Raton, FL, 1995, Vol. III.
[5] R.E. March, J. Mass Spectrom. 32 (1997) 351.
[6] G. Lawson, R.F. Bonner, J.F.J. Todd, J. Phys. E 6 (1973) 357.
[7] R.F. Bonner, G. Lawson, J.F.J. Todd, Int. J. Mass Spectrom. Ion Phys. 10 (1972/73) 197.
[8] J.F.J. Todd, Mass Spectrom. Rev. 10 (1991) 3.
[9] F. Vedel, J. Andre, M. Vedel, G. Brincourt, Phys. Rev. A 27 (1983) 2321.
[10] R.K. Julian, R.G. Cooks, Anal. Chem. 65 (1993) 1827.
[11] S. Guan, A.G. Marshall, Anal. Chem. 65 (1993) 1288.
[12] C.D. Hanson, M.E. Castro, E.L. Keley, D.H. Russell, Anal. Chem. 62 (1990) 1352.
[13] J.T. Tape, P.T. Smith, Phys. Rev. 46 (1934) 773.
[14] J. Andre, Thesis, Université de Provence, Marseille, France, 1978.
[15] M. Splendore, F.A. Londry, R.E. March, R.J.S. Morisson, P. Perrier, J. Andre, Int. J. Mass Spectrom. Ion Processes 156 (1996) 11.
[16] J.E.P. Syka, W.J. Fies, Proceedings of the 35th ASMS Conference on Mass Spectrometry, Denver, CO, May 1987, p. 767.
[17] R.G. Cooks, C.D. Cleven, L.A. Horn, M. Nappi, C. Weil, M.H. Soni, R.K. Julian Jr., Int. J. Mass Spectrom. Ion Processes 146/147 (1995) 147.
[18] S.A. Lammert, C.D. Cleven, R.G. Cooks, J. Am. Soc. Mass Spectrom. 5 (1994) 29.
[19] Y. Zerega, J. Andre, G. Brincourt, R. Catella, Int. J. Mass Spectrom. Ion Processes 132 (1994) 67.
[20] Y. Zerega, J. Andre, G. Brincourt, R. Catella, Int. J. Mass Spectrom. Ion Processes 132 (1994) 57.
[21] P. Perrier, T. Nguema, M. Carette, J. Andre, Y. Zerega, G. Brincourt, R. Catella, Int. J. Mass Spectrom. Ion Processes 171 (1997) 19.
[22] Y. Zerega, J. Andre, G. Brincourt, R. Catella, Int. J. Mass Spectrom. Ion Processes 135 (1994) 155.